Express Polymer Letters Vol.20, No.6 (2026) 594–616
Available online at www.expresspolymlett.com
https://doi.org/10.3144/expresspolymlett.2026.45

Research article

Dynamic mechanical and spectroscopic studies of soy flour adhesives

Anthony Allen Parker[1*], *Joseph John Marcinko*[2]

[1]A. A. Parker Consulting, LLC, Lakewood Ranch, FL 34202, USA
[2]Polymer Synergies, LLC, Bradenton, FL 34211, USA

Received 20 November 2025; accepted in revised form 2 April 2026

Abstract. We used dynamic mechanical analysis (DMA) to evaluate soy flour adhesives made with and without a conventional crosslinking agent, polyamideamine-epichlorohydrin (PAE). Fixed-frequency and constant strain rate studies revealed that PAE contributes to a decrease in glass transition temperature (T_g), an increase in toughness, and a decrease in both the rubbery plateau modulus and onset temperature, consistent with plasticization. Fourier transform infrared spectroscopy (FTIR) and nuclear magnetic resonance (NMR) studies of water-soluble extracts from pre-cured soy flour revealed the presence of polypeptides with exchangeable protons, carbohydrates, citric acid and lactic acid. Deuterium exchange studies showed that the protonated peptides were no longer water-soluble after cure. Instead, post-cure extracts contained heat-modified carbohydrates and carboxylic acids, together with adipic acid when PAE was employed. These results are consistent with a mechanism whereby PAE not only undergoes hydrolysis and chain scission, but also competitively co-reacts with peptides and carboxylic acids to yield a plasticized chain-extended network with decreased crosslink density, counter to its anticipated function. The implications of these findings as they pertain to moisture resistance and wood adhesion will be discussed.

Keywords: *biopolymer, dynamic mechanical analysis, carbohydrates, toughness, hydrolysis, plasticizer, spectroscopy*

1. Introduction

Although soy flour adhesives are desirable for reasons pertaining to economics and sustainability, they have found only limited utility in the wood composites industry owing to their poor moisture resistance [1], especially when compared to other types of conventional synthetic adhesives like phenol formaldehyde resins (PF) and polymeric methylenediphenyl diisocyanate (PMDI) resins, both of which are known for their use in the manufacture of weather-resistant wood composites [2]. The moisture resistance of soy flour adhesives has been improved with modifiers like magnesium oxide [3] and polyamideamine-epichlorohydrin (PAE) [4], but even these types of modifications have fallen short when it comes to providing the degree of moisture resistance that is required for more stringent applications.

It has been recognized that adhesives containing more expensive soy protein isolates (SPIs) provide better moisture resistance than those made from soy flour [1, 5], primarily due to their higher levels of protein and lower levels of moisture-sensitive carbohydrate sugars [1, 5, 6]. Moreover, the moisture resistance of SPI adhesives has been observed to improve when the native proteins become denatured with heat, leading to the exposure of water-resistant hydrophobic protein moieties [5, 7]. This suggests that the performance of soy-based composites might be further improved though the use of SPIs in place of soy flour, coupled with higher processing temperatures and/or with longer dwell times during processing.

However, for reasons pertaining to economics, industries are consistently striving to optimize and

*Corresponding author, e-mail: tony@aaparkerconsulting.com

reduce manufacturing costs. This equates to preferences for cheaper materials like soy flour over SPIs [1, 7], as well as to a universal preference for high throughput rates, low process temperatures, and short process dwell times, regardless of adhesive type. Consequently, if soy flour adhesives are to become economically viable alternatives to better-performing resins like PMDI and PF [1, 2], they will need to provide equivalent or better performance with minimal impact on manufacturing costs, even if this necessitates the use of process conditions that fall short of those needed for full soy protein denaturation [5].

Published accounts have revealed that soy flour contains a variety of polypeptides and carbohydrates [1, 6]. Moreover, it has been hypothesized that carbohydrates might somehow interfere with the wet strength of soy flour adhesives [7]. In our previous study of plywood composites made with water-borne soy flour adhesives [8], we observed that when poplar laminates are press-laminated under mild process conditions (*i.e.*, simulating conventional high throughput rates), water-soluble carbohydrate components undergo partitioning during the wood lamination process, and become concentrated at the adhesive–wood interface, independently of the presence of PAE. Moreover, the locus of moisture-induced delamination was also observed to be associated with the failure of this layer, independently of the presence of PAE, posing the possibility that the improvement in wet-strength adhesion from PAE [1, 4, 5, 7] might be related to PAE-induced mechanical property differences within the bulk adhesive rather than to PAE-induced compositional differences within the weak boundary layer. One of the objectives of the present study is to test this hypothesis.

In addition, we also hypothesized that the moisture resistance of wood laminates might be improved by crosslinking the moisture-sensitive interfacial boundary layer [8] through judicious choices of alternative co-reactants. In this way, the soy system might be made to behave more analogously to conventional moisture-resistant systems like those made from PF and PMDI, both of which are known to penetrate the adherends and then to undergo in-situ chemical crosslinking to yield moisture resistant interphases comprised of wood components and polymer [9, 10]. Thus, by gaining a better understanding of the structures and potential reactivities of the water-soluble components in soy flour, we have reasoned that it should become possible to create more moisture-resistant versions of soy-based adhesives [8], and perhaps to eliminate the moisture-sensitive weak boundary layer altogether. Hence, a second objective of the present study is to characterize the water-soluble components not only for the purpose of studying the mechanism of PAE's interaction with soy flour, but also for the purpose of identifying the types of functionalities that might be available to participate in facile network-forming reactions with alternative crosslinking agents.

2. Experimental

2.1. Sample preparation

Using procedures outlined previously [8], we prepared monolithic soy adhesive films from dispersions of soy flour (Prolia 200/70 mesh/PDI soy flour, Cargill Inc., Minneapolis, MN, USA) in water, with and without polyamideamine-epichlorohydrin (PAE) resin (CA-1130 PAE, 30% w/w in water, Solenis LLC, Wilmington, DE, USA). Note that 200-mesh equates to an average soy flour particle size of 74 μm, and PDI is the protein dispersibility index, which relates to the fraction of water-soluble proteins and to how well the soy flour disperses in water. One of the dispersions (labeled 67-3) was prepared by mixing the 30% solids PAE solution (w/w) with a premixed dispersion of soy flour in water to yield a final composition comprising 38% total solids (w/w) in water, where the effective ratio of soy flour to PAE was 96/4 (w/w) on a solids basis. A second dispersion without PAE (labeled 67-4) was prepared by mixing neat soy flour in water to yield a composition with the same percentage of solids in water (*i.e.*, 38% w/w). The total weight of each dispersion was approximately 280 g.

In the next step, monolithic films were prepared by smearing the water-borne dispersions between two layers of nonporous aluminum foil, and then by pressing the samples in a hot press (Carver Auto Series 13.6 Metric-Ton Laboratory Press, Carver, Inc., Wabash, IN, USA) at a temperature of 130 °C, and under 1055 kPa pressure for a 4 min dwell time. Five replicate films were pressed from each 280 g aliquot of dispersion to a thickness of approximately 0.6 to 0.8 mm. After pressing, the upper foil layer was peeled away, and the adhesive films were placed in a 130 °C gravity oven for an additional 10 min to assist in the removal of residual moisture. These films were made under temperature conditions that mimic those typically used to manufacture wood composites, but

without the wood [8]. The final solid films were homogeneous and opaque in appearance, and consisted of 96/4 w/w soy flour/PAE (sample 67-3), and 100% soy flour (sample 67-4).

Note that the 67-3 and 67-4 films were replicates of those made in our previous study [8], where we found that water-soluble components from the adhesives produced a moisture-sensitive weak boundary layer that became the locus of moisture-induced delamination failures in laminated wood composites, independently of the presence of PAE, and where solid-state nuclear magnetic resonance (NMR) studies showed that the molecular mobility of soy flour was enhanced by the presence of PAE [8]. In the present study, the 67-3 film with PAE was qualitatively observed to be less stiff and more ductile than the comparative 67-4 film without PAE. We observed the same qualitative trend in our previous study [8].

In addition to the two types of hot-pressed water-borne films, two comparative dry-blend samples were also made, one with PAE and one without PAE. In the first case, the 30% aqueous solution of PAE was mixed with dry soy flour powder, which resulted in a dry composition that was equivalent to that of the comparative hot-pressed water-borne film, 67-3 as described above (*i.e.*, 96/4 w/w soy flour components and PAE components). In the second case, 97 parts of dry soy flour powder were mixed with 3 parts by weight water to yield a dry blend with a water-add that was like that of the dry-blend sample containing the 30% PAE solution. The resulting neat dry blend was analogous to the hot-pressed water-borne film, 67-4. The two comparative dry blends were hot-pressed under the same conditions as the water-borne films to yield homogeneous solid samples having a thickness ranging from approximately 0.6 to 0.8 mm. Unlike the opaque films that were formed from the hot-pressing of water-borne dispersions, the hot-pressed dry blends were amber and translucent. The dry blends also exhibited a noticeable degree of thermoplastic flow under pressure, with the 96/4 w/w soy flour/PAE sample flowing to a greater degree than the neat soy flour sample. The resulting 67-3 dry-blend sample was qualitatively observed to be less stiff and more ductile than the comparative 67-4 dry-blend sample, as was similarly observed upon comparison of the analogous hot-pressed water-borne films.

2.2. Dynamic mechanical analysis (DMA)

Single samples of the solid monolithic films (*i.e.*, those that were hot-pressed from aqueous water-borne dispersions) were analyzed with a TA Instruments Discovery 850 dynamic mechanical analyzer (TA Instruments, New Castle, DE, USA) at the University of Maine advanced structures and composites center in Orono, Maine (USA). Individual samples were run in tensile mode at a fixed frequency of 1 Hz from –80 to 175 °C at a heating rate of 5 °C/min, with an oscillation strain amplitude of 0.01%. Sample dimensions were approximately 0.6 mm thickness, 1.0 cm width, and 2 cm length. A low strain amplitude was employed to stay within the linear region of viscoelasticity (*i.e.*, to minimize permanent deformation).

In separate experiments, the DMA was set up to run at a constant strain rate in 3-point bending mode. In this experiment, single samples of the hot-pressed dry blends were run isothermally at 30 °C with a constant strain rate of 0.025%/s to the point of failure. The dimensions of the samples were fixed: span length was 10.0 mm, width was 5.3 mm, and thickness was 0.668 mm. The stress and strain were recorded as a function of time up to the ultimate point of sample failure.

2.3. Water extraction

With the use of procedures like those outlined previously [8], specimens of as-received soy flour and the solid adhesive films that were hot-pressed from water-borne dispersions were individually subjected to a water extraction protocol for the purpose of removing water-soluble components. Replicates of pressed films, representative of each adhesive type, were crushed and mixed. Approximately 1 g aliquots of the crushed films were separately placed into individual centrifuge tubes together with 11 g of pH-neutral distilled water per tube (six tubes per sample type). The same procedure was followed for as-received soy flour powder. The individual tubes were shaken by hand and were placed into a static gravity oven for ~10 h at 45–50 °C, which assisted in the dissolution of water-soluble components. After the soak period, the tubes were centrifuged under ambient conditions for 30 min at 3400 rpm. The liquid supernatants were then decanted into new centrifuge tubes, which were centrifuged for an additional 1.5 h under ambient conditions. The clear supernatant solutions

were then decanted into individual glass jars for subsequent drying at 45–50 °C for 48 h. The extracts from as-received soy flour and from the 67-3 adhesive (cured with PAE) dried to form clear, low-haze films. By contrast, the crude extract from the hot-pressed sample 67-4 dried to yield an opaque hazy film.

2.4. Reconstitution in aqueous media

In subsequent steps, aliquots of the dried extracts were reconstituted in distilled H_2O, and separately in D_2O (Aldrich, 99.9% D, cat. #151882, St. Louis, MO, USA). Upon reconstitution, the low-haze extracts from as-received soy flour and from the 67-3 adhesive were observed to form clear solutions. By contrast, the hazy extract from 67-4 underwent separation to yield a clear supernatant with well-dispersed white particulates. Each of the H_2O- and D_2O-reconstituted extracts were individually filtered through Millex GP 22-micron filters from Millipore (Burlington, MA, USA), and the clear filtrates were transferred via syringe to separate glass jars. The filtered aqueous solutions were then used for nuclear magnetic resonance (NMR) analyses, and the remaining aliquots were dried at 45–50 °C for subsequent solid-state Fourier transform infrared spectroscopy (FTIR). Samples of the remaining white sediment from the 67-4 crude extract were washed separately with H_2O and D_2O. The washed sediments from the reconstituted 67-4 extracts were then dried at 45–50 °C for FTIR analysis.

2.5. FTIR studies

Solid-state surface attenuated total reflectance FTIR (SATR-FTIR) studies were performed with a Bruker Alpha-P spectrometer (Bruker Instruments, Billerica, MA, USA) equipped with a diamond-cell attenuated total reflectance (ATR) accessory. Anvil pressure was applied to ensure intimate contact between the samples and the diamond crystal. Single-bounce spectra, referenced against atmospheric background spectra, were obtained under ambient conditions by averaging the signals of 36 scans at 2 cm^{-1} resolution over the spectral range 4000 to 650 cm^{-1}. Solid samples of the oven-dried extracts were evaluated after reconstitution in H_2O, and after reconstitution in D_2O to probe for the possibility of deuterium exchange.

2.6. Solution NMR studies

Nuclear magnetic resonance (NMR) studies were conducted at the advanced magnetic resonance imaging and spectroscopy (AMRIS) facility at the University of Florida (Gainesville, FL, USA) with a 600 MHz Bruker Neo 600 console with an 89 mm bore, equipped with a 5 mm BBOF cryoprobe (Bruker Instruments, Billerica, MA, USA). Signal-averaged one-dimensional proton (^1H) solution spectra were acquired at 25 °C along with several two-dimensional spectra [11], including proton homonuclear correlated spectra (^1H–^1H COSY), heteronuclear single quantum coherence spectra (^1H–^{13}C HSQC) and heteronuclear multiple quantum coherence spectra (^1H–^{13}C HMBC). The spectra were acquired with the use of the reconstituted and filtered D_2O solutions (~9% w/w extracted solids) from the as-received soy flour extract, from the 67-3 extract and from the 67-4 extract. Specific spectral regions associated with key components were analyzed separately, including the region associated with anomeric carbohydrate protons (HSQC, ^1H 2.7–5.7 ppm coupled to ^{13}C 55–105 ppm) [12], the region associated with citric acid (HSQC and HMBC, ^1H 2.58–3.80 ppm coupled to ^{13}C 30–190 ppm), the region associated with lactic acid (HSQC and HMBC, ^1H 0.76–1.50 ppm coupled to ^{13}C 0–220 ppm) and the region associated with adipic acid (COSY, HSQC and HMBC). Spectral assignments for citric, lactic and adipic acid were individually corroborated by chemical shift calculations that were performed with the ChemDraw Ultra 11.0 software from CambridgeSoft (Cambridge, MA, USA), and with data from the Human Metabolome Database [13]. In addition, the presence of citric acid was confirmed through analysis of a citric acid reference solution (Aldrich, 99.5%, 192 /mole, cat. # 251275, St. Louis, MO, USA).

In separate solution NMR experiments, spectra were acquired at 25 °C with a 600 MHz Bruker Bio-Spin Avance III HD spectrometer with a 54 mm bore, equipped with a 5 mm TXI CryoProbe (Bruker Instruments, Billerica, MA, USA). ^1H spectra were acquired from two separately filtered aqueous solutions, one in D_2O and one in H_2O/D_2O (93/7 w/w), with each containing 6% w/w of the reconstituted as-received soy flour extract. The purpose of these one-dimensional ^1H NMR experiments was to test for the

presence of exchangeable protons in the as-received soy flour extract. Water suppression techniques were used in the presence of H_2O. In addition, a one-dimensional ^1H NMR spectrum was generated from a 2D ^1H–^{15}N HSQC experiment [11], with H_2O/D_2O (93/7 w/w) as the solvent. The purpose of this experiment was to probe for the presence of water-soluble, protonated nitrogen species (*e.g.*, soluble peptides). The nitrogen transmitter frequency was centered near 75 ppm, specifically for the purpose of detecting both static and exchangeable protons bonded to amine and amide nitrogen centers.

3. Results and discussion

3.1. Overview of NMR results

^1H NMR spectra of the filtered water-soluble extracts are provided in Figure 1. The region between 0.5 and 5.5 ppm shows some of the key differences between the water-soluble reactants (*i.e.*, the as-received soy flour extract) and reaction products. Visual inspection reveals the presence of new anomeric carbohydrate protons in both 67-3 and 67-4, protons associated with lactic acid and citric acid in all three extracts, protons consistent with adipic acid in 67-3, and process-induced changes in line widths and relative intensities. Further details on spectral assignments and mechanisms will be discussed below.

3.2. Carbohydrate chemistry

Independent of the presence or absence of PAE, the thermal curing process changed the carbohydrate compositions of the water-soluble fractions, as evidenced by a change in the FTIR C–O stretching region [8] between 850 and 1200 cm^{-1} (Figure 2), and as evidenced by a change in the ^1H–^{13}C HSQC spectra, which showed the formation of new anomeric and non-anomeric protons that were not present in the extracts from as-received soy flour (Figure 3). Soy flour has been reported to contain about 51% protein and 34% carbohydrates by weight [6], so it is plausible that at least a portion of the water-soluble carbohydrates have undergone Maillard reactions with peptides under the thermal process conditions used in this study [14]. Indeed, such reactions have previously been observed to influence the ^1H NMR fingerprint spectra for glycosidic anomeric protons and non-anomeric protons in other polysaccharides [15]. Importantly, however, regardless of the reasons for these types of changes, the resulting carbohydrates remained water-soluble after thermal processing, independently of the use of PAE. This finding remains consistent with prior studies [8], where similar C–O stretching bands consistent with carbohydrates were observed to appear in association with water-soluble components at the wood/soy-adhesive interface, independent of the presence or absence of PAE; and where solid-state ^{13}C NMR spectra revealed the presence of an anomeric carbon centered near 93 ppm in identically pressed films, which disappeared upon water extraction of the films [8].

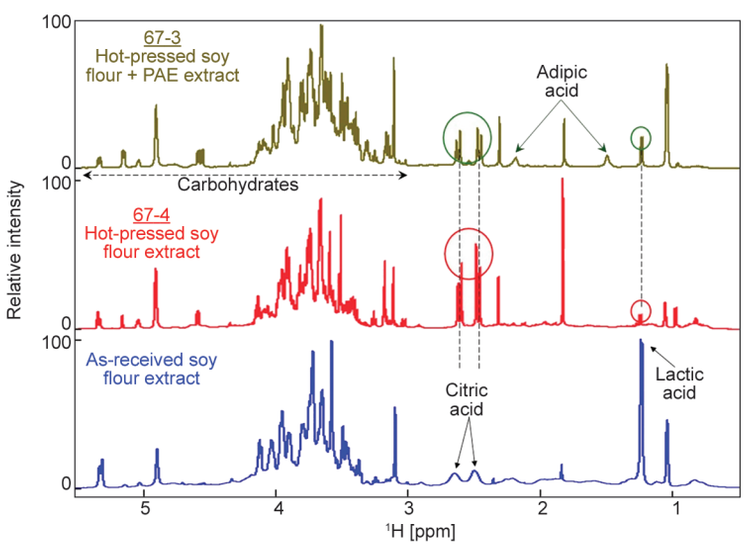

Figure 1. Stacked overlay of ^1H solution NMR spectra denoting key differences between the low-haze water-soluble extracts (5.5 to 0.5 ppm). Samples were reconstituted in D_2O and filtered (~9% w/w solids in solution). Intensities were normalized to a common vertical scale for relative comparisons.

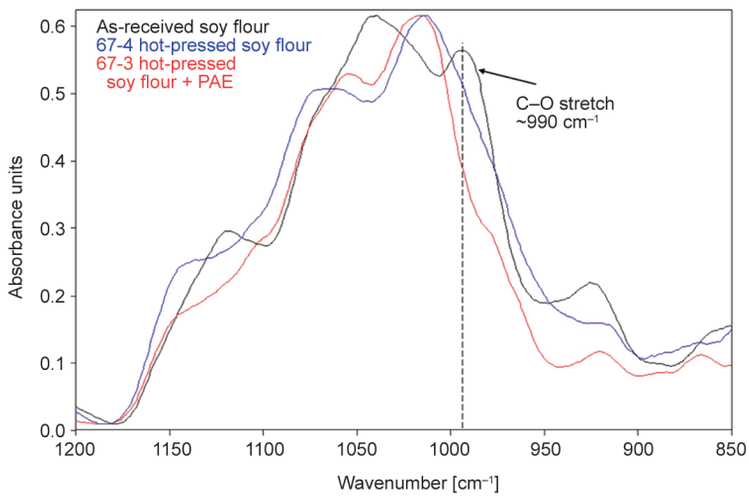

Figure 2. SATR-FTIR over the spectral range 850 to 1200 cm^{-1} illustrating the differences in the C–O stretch region associated with water-soluble carbohydrates [8, 16]. The films were cast and dried from low-haze water-soluble/filtered extracts after reconstitution in H_2O. Spectra were vertically maximized to a common scale.

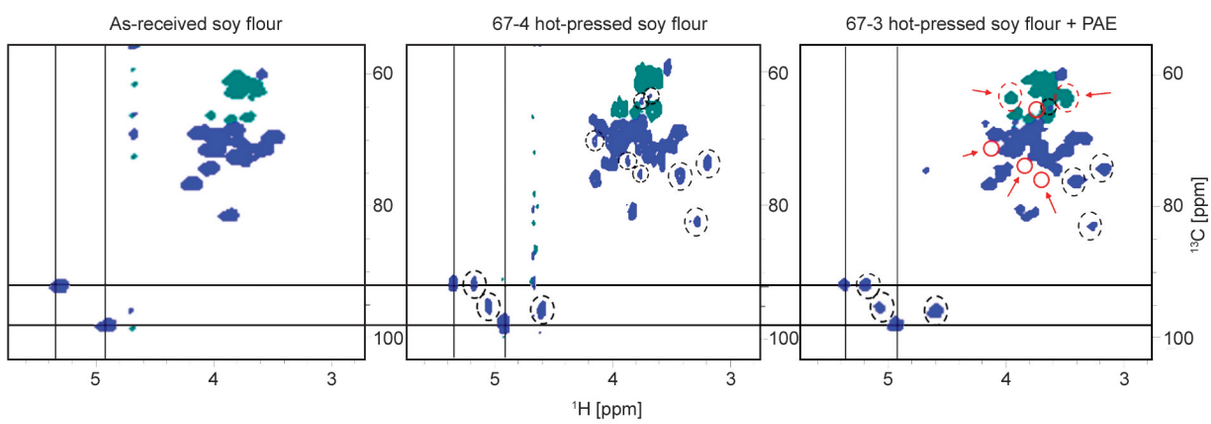

Figure 3. Two-dimensional ^{1}H-^{13}C HSQC solution spectra over the region associated with anomeric carbohydrate protons (*i.e.*, ^{1}H 2.7–5.7 ppm to ^{13}C 55–105 ppm). The low-haze extracts were reconstituted in D_2O and filtered (~9% w/w extracted solids in solution). Solid lines delineate cross peaks for anomeric protons that remain unchanged. Green cross peaks represent aliphatic methylene protons. Cross peaks circled with black dashed lines represent new anomeric protons from hot-pressing, independent of PAE. Red solid circles represent cross peaks that were diminished in the presence of PAE, and red dashed circles represent new cross peaks in the presence of PAE.

3.3. Thermally induced reaction chemistry in the presence and absence of PAE

Thermal history was also observed to influence the solid-state FTIR absorption characteristics of amide-carbonyl components. As shown in Figure 4, the as-received soy flour extract, and the crude extract from 67-4 shared a common absorption band at ~1640 cm^{-1}. This band appeared as a distinct shoulder, adjacent to a higher intensity band, centered near 1582 cm^{-1} in the as-received soy flour extract, and centered near 1568 cm^{-1} in the crude 67-4 extract. These bands are consistent with the types of amide-I and amide-II carbonyl bands that are associated with polypeptides [16]. By contrast, a new higher-intensity shoulder band appeared at ~1608 cm^{-1} in the low-haze extract from the PAE-cured adhesive (67-3), adjacent to a second band centered near 1582 cm^{-1}. Unlike the analogous crude 67-4 extract, the 67-3 extract was completely water-soluble, and there was no evidence of a high-haze component with an amide-I band at 1640 cm^{-1}.

Upon filtering and separating the crude 67-4 extract into its low-haze and high-haze components, the amide-I band at 1640 cm^{-1} was absent from the soluble low-haze component. Instead, it was contained exclusively within the 67-4 high-haze component (Figure 5). Consequently, the water-soluble carbonyl amide that was originally present in the as-received soy flour was thermally transformed to yield an insoluble proteinaceous reaction product with the same

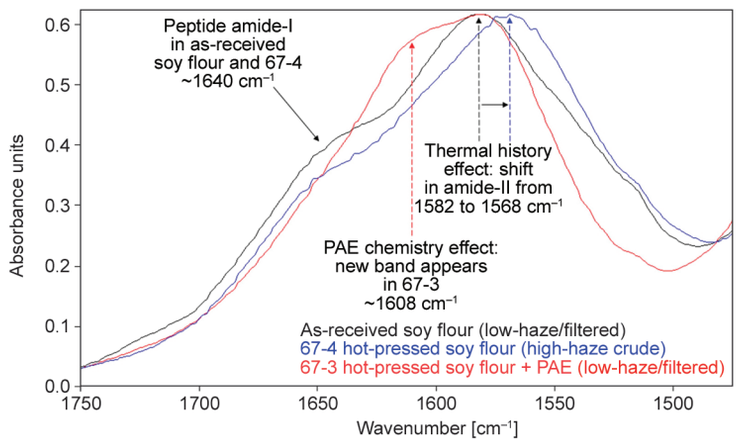

Figure 4. SATR-FTIR over the spectral range 1475 to 1750 cm^{-1} illustrating differences in the carbonyl stretch region [16]. The films were cast and dried from extracts after reconstitution in H_2O. Spectra were vertically maximized to a common scale.

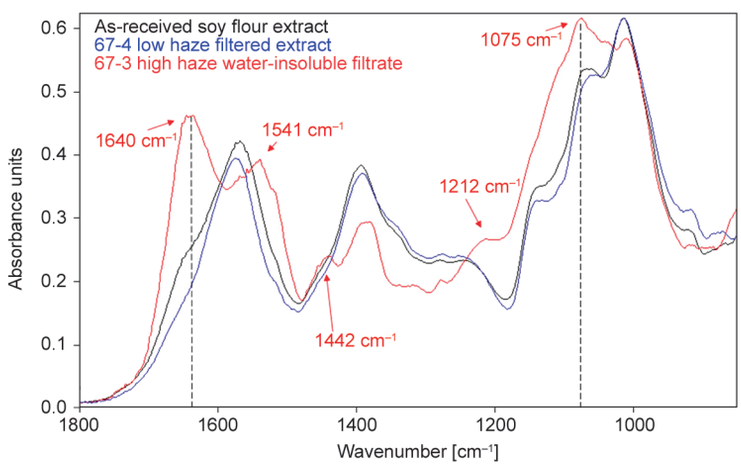

Figure 5. We performed and evaluated SATR-FTIR over the spectral range of 950 to 1800 cm^{-1} to determine the effects of thermal history (hot-pressed 67-4) on the transformation of water-extractable components from as-received soy flour (*i.e.*, amide and carbohydrate) into an insoluble reaction product. The materials were cast and dried from extracts after reconstitution in H_2O. Spectra were vertically maximized to a common scale.

characteristic amide-I band at 1640 cm^{-1}, and with additional absorption bands appearing at 1541, 1442, 1212 and 1075 cm^{-1}, suggesting the possible formation of a Maillard reaction product [14].

3.4. Deuterium exchange experiments

Given that the soy flour used in this study was characterized with a PDI of 70, it is reasonable to expect that a fraction of the proteins would be soluble in water, and that some would contain reactive side-chain residues [1, 17]. In fact, the presence of water-soluble peptides was confirmed via ^1H NMR experiments as shown in Figure 6 and Figure 7. Figure 6 displays the ^1H chemical shift region associated with amides, amines, and other types of protons (*e.g.*, hydroxyls) for the as-received soy flour extract in D_2O (top), and in H_2O (bottom); and Figure 7 displays the same spectrum for the as-received soy flour extract in H_2O (top) together with the ^1H axis from a 2D ^1H–^{15}N HSQC experiment (bottom).

In solution NMR, all exchangeable protons will become fully exchanged with deuterium in D_2O (*e.g.*, protons from primary amines, secondary amines, amides, hydroxyls, *etc.*) and will therefore not appear in the resulting ^1H NMR spectrum. By contrast, in the presence of H_2O, exchangeable protons can exchange freely in equilibrium with the solvent medium and will therefore appear as broad peaks that would otherwise be absent from the analogous spectrum in D_2O [16, 18]. These types of differences were indeed observable as shown in Figure 6, where at least three resonance peaks that were absent in the D_2O spectrum became visible in the presence of water (*i.e.*, a broad peak centered near

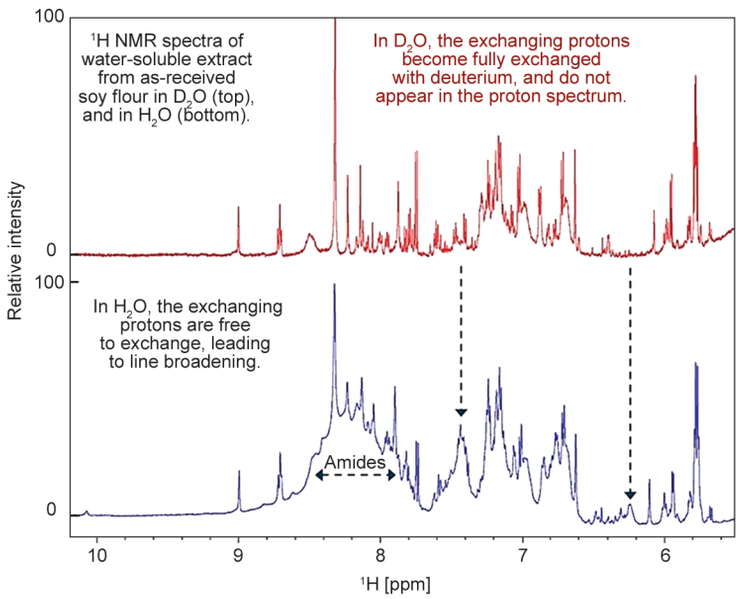

Figure 6. Stacked ^{1}H NMR spectra of the water-soluble extract from as-received soy flour reconstituted in D_2O (top) and in H_2O (bottom). Intensities were normalized to a common vertical scale for relative comparisons.

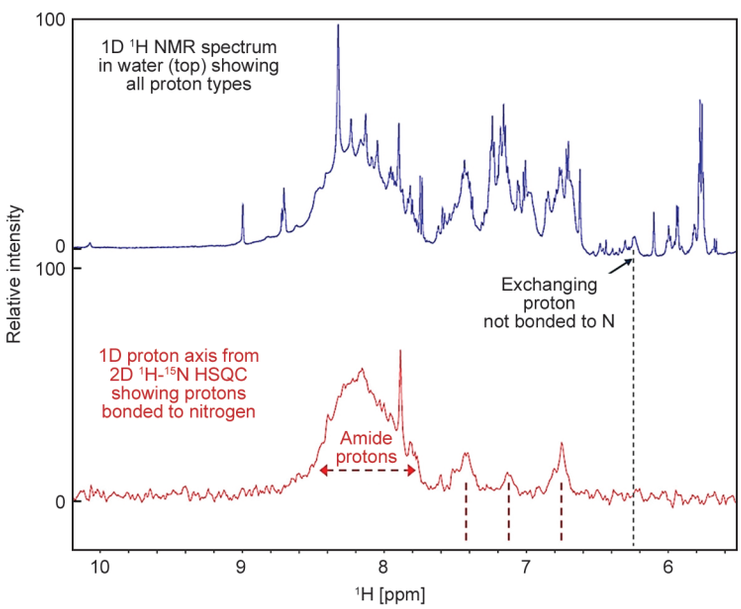

Figure 7. Stacked NMR spectra of the water-soluble extract from as-received soy flour reconstituted in H_2O showing the standard ^{1}H NMR spectrum (top), and the ^{1}H axis from 2D ^{1}H-^{15}N HSQC. Intensities in the top spectrum were normalized, and the intensities in the bottom spectrum were normalized to the top spectrum with the broad peak centered near 8.2 ppm.

8.2 ppm, a peak near 7.4 ppm, and a peak near 6.2 ppm).

The ^{1}H spectrum from the 2D ^{1}H–^{15}N HSQC experiment as presented in Figure 7 confirms that several protons were bonded to nitrogen, including three non-exchanging types at 7.9, 7.15, and 6.75 ppm, and two exchangeable types at 8.2 and 7.4 ppm. Note that the exchanging proton centered near 6.2 ppm was not present in the 2D ^{1}H–^{15}N HSQC, which indicates that this proton was bonded to a different type of nucleus, such as oxygen.

Because of the low natural abundance of ^{15}N (~0.38%) compared to ^{1}H nuclei (100%), the resolution of ^{15}N resonances was not high enough for us to make use of 2D cross-correlations to assist with N–H structural assignments. However, the ^{1}H resolution was sufficient to allow for the proposal of structures based on known ^{1}H chemical shifts for peptides and amino acid side chains residues. For example, the broad resonance centered at ~8.2 ppm is consistent with the presence of exchangeable, hydrogen-bonded, secondary amide protons, like those

comprising the amide backbone of water-soluble polypeptide chains [19]. Indeed, this finding corroborates the appearance of the band at 1640 cm^{-1} in the FTIR spectrum of the as-received soy flour extract, consistent with an amide carbonyl stretch [16].

It is also plausible that the other types of nitrogen-bound protons could be associated with amino acid side chain residues (*e.g.*, primary, and/or secondary amines). For example, the ^1H resonance at 7.9 ppm could be consistent with the hydrogen bonded indole N–H of tryptophan, and/or with the imidazole N–H of histidine, both of which are water-extractable components in soy protein isolates [20]. The ^1H resonance at 7.4 ppm could also be consistent with the hydrogen-bonded imidazole N–H of histidine. In addition, the peaks at 7.15 and 6.75 ppm could be consistent with the H-bonded $–NH_2$ side chains of arginine, asparagine, or lysine, all of which are also known to be water-extractable components of soy flour [20].

Deuterium exchange studies with FTIR provided additional confirmation of the presence of primary amines and/or secondary amides within the as-received soy flour extract. As shown in Figure 8, when the water-soluble extract from soy flour was reconstituted in D_2O, a new absorption band appeared near 2475 cm^{-1}. This band was absent when the extract was reconstituted in H_2O.

Upon deuteration, N–H stretching frequencies are known to shift downward by a factor of ~1.34 due to the increased reduced mass of the N–D bond compared to the N–H bond [21]. Thus, for an amine with an N–H stretch from about 3280 to 3320 cm^{-1}, the corresponding N–D stretch would occur at about 2450 to 2475 cm^{-1}. Hence, the appearance of the absorption band centered near 2475 cm^{-1} is consistent with an N–D stretch from deuterium exchange, which corroborates with the solution NMR results. By contrast, as shown in Figures 9 and 10, when the low-haze extracts from the hot-pressed films were reconstituted in D_2O, the N–D stretching band centered near 2475 cm^{-1} was not present. When combined with the disappearance of the amide-I carbonyl band, the absence of exchangeable protons supports the hypothesis that the water-soluble polypeptide components were not present in the low-haze extracts from 67-3 and 67-4. Instead, the polypeptides were transformed with heat to yield one or more insoluble reaction products.

These results collectively show that the water-soluble peptides in soy flour contain reactive, exchangeable protons. Consequently, it is not surprising that these components underwent thermally induced reactions, particularly given the presence of co-reactants like water-soluble carbohydrates and PAE. For example, as discussed in the previous section, water-soluble carbohydrates can react with water-soluble peptides via a Maillard reaction [14], which could account for the new anomeric protons that were observed to be present in the water-soluble extracts from 67-3 and 67-4. In addition, a reaction between water-soluble peptides and carbohydrates could also lead to water-insoluble proteinaceous reaction products, like that which was isolated from the crude 67-4 extract.

3.5. Lactic acid and citric acid

Condensation reactions could also occur between water-soluble soy flour peptides and other types of

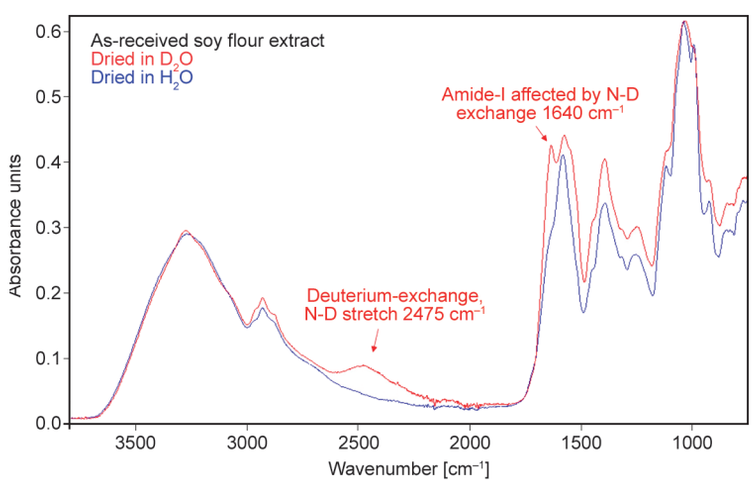

Figure 8. SATR-FTIR over the spectral range of 750 to 3800 cm^{-1} for the as-received soy flour extract, cast and dried from low-haze filtered extracts reconstituted in H_2O and D_2O. Spectra were vertically maximized to a common scale.

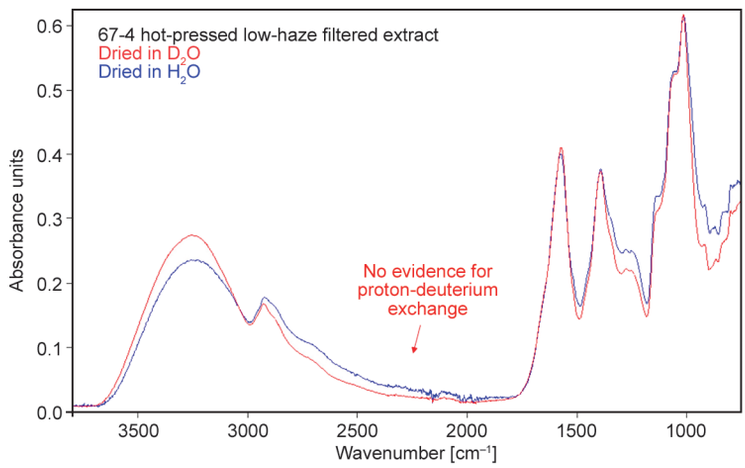

Figure 9. SATR-FTIR over the spectral range of 750 to 3800 cm^{-1} for the extract from 67-4 (neat, hot-pressed soy flour), cast and dried from low-haze filtered extracts reconstituted in H_2O and D_2O. Intensities were vertically maximized to a common scale.

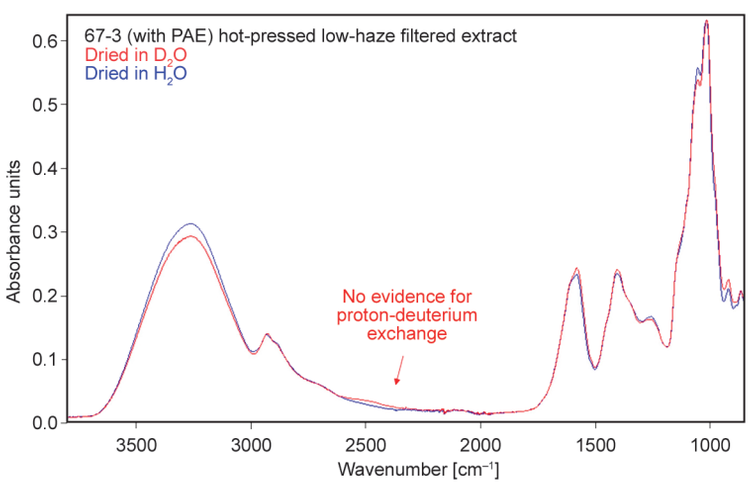

Figure 10. SATR-FTIR over the spectral range of 750 to 3800 cm^{-1} for the extract from 67-3 (hot-pressed soy flour with PAE), cast and dried from low-haze filtered extracts reconstituted in H_2O and D_2O. Intensities were vertically maximized to a common scale.

water-soluble components that were present in as-received soy flour, including components like lactic acid and citric acid. The respective ^{1}H peak assignments for these compounds were confirmed by 2D ^{1}H–^{13}C HSQC and HMBC NMR experiments as shown in Figures 11 and 12, respectively.

Lactic acid can form via carbohydrate fermentation, which can occur when soy flour is dispersed in water [22]. Thus, it is plausible that lactic acid could have been formed during the initial preparation of the soy flour dispersions in water, and/or during the water-extraction process. By contrast, citric acid is not indigenous to soy, so its presence is likely associated with its use as an additive, perhaps to enhance shelf stability and flavor in food-grade soy [23, 24]. However, as it pertains to adhesive chemistry, citric acid can also function as a metal chelating agent [24], and it can also react with protein hydroxyl groups leading to protein and cellulose crosslinking [25–27]. Citric acid can also lead to carbohydrate crosslinking [28].

Note that the absence of a free carboxylic acid carbonyl stretch in each of the solid FTIR spectra implies that the two acids exist as carboxylate salts in the solid-state films. The free carboxylic acid stretch vibration is known to occur near 1700–1710 cm^{-1}, while the asymmetric carbonyl stretch for a carboxylate salt is known to occur at lower wavenumbers [16]. This can lead to an overlap with the absorbance region that is commonly associated with amide-II absorption bands [16], thereby making it difficult to discern their presence with FTIR alone. In fact, it is likely that the absorption bands between 1540 and 1608 cm^{-1} (as noted in the previous section) contain overlapped contributions from each of the two carboxylate salts.

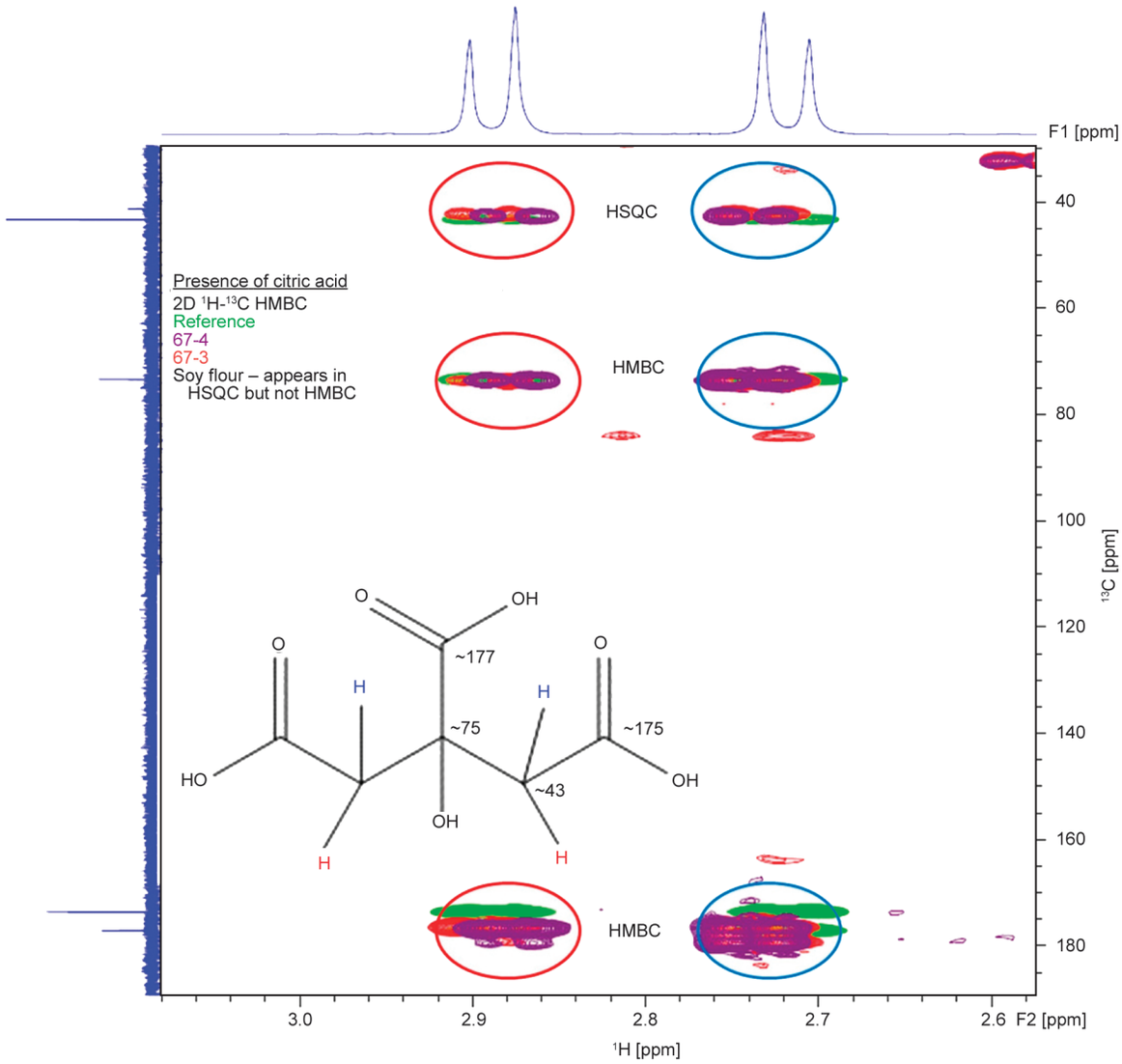

Figure 11. 2D ^{1}H–^{13}C HMBC with bleed-through from HSQC (top cross-peaks) as observed for a citric acid reference compound and for all three extracts. The cross-peak assignments are color coded to represent each extract, and each cross-peak is circled with a color code corresponding to the blue and red color-coded protons as denoted within the structure inlay.

Regarding the possibility of reactions between either citric acid and/or lactic acid with other water-soluble components, the formation of water-soluble citrate or lactate esters can be ruled out because of the absence of an ester carbonyl absorption band in the FTIR region near 1730 cm^{-1} [16]. However, as shown in Figure 1, the ^{1}H NMR peaks associated with lactic acid exhibited lower relative intensities after hot-pressing, implying that lactic acid may have been consumed to yield water-insoluble reaction products.

It is plausible that that lactic acid could have been consumed during hot-pressing through reactions with proteins [22]. If so, the resulting reaction products could have been rendered water-insoluble, in which case they would not be present in the water-soluble extracts from the hot-pressed adhesives. This would account for the observed decrease in ^{1}H peak intensities.

Like lactic acid, the ^{1}H NMR peaks for citric acid also underwent spectral changes after hot-pressing. However, unlike the aliphatic ^{1}H peaks for lactic acid, the citric acid peaks underwent line narrowing. Prior to hot-pressing, the citric acid peaks in the as-received soy flour extract were selectively line-broadened, while the surrounding ^{1}H NMR peaks (*e.g.*, those of lactic acid and carbohydrates) exhibited narrower line widths (Figure 1). After hot-pressing, the

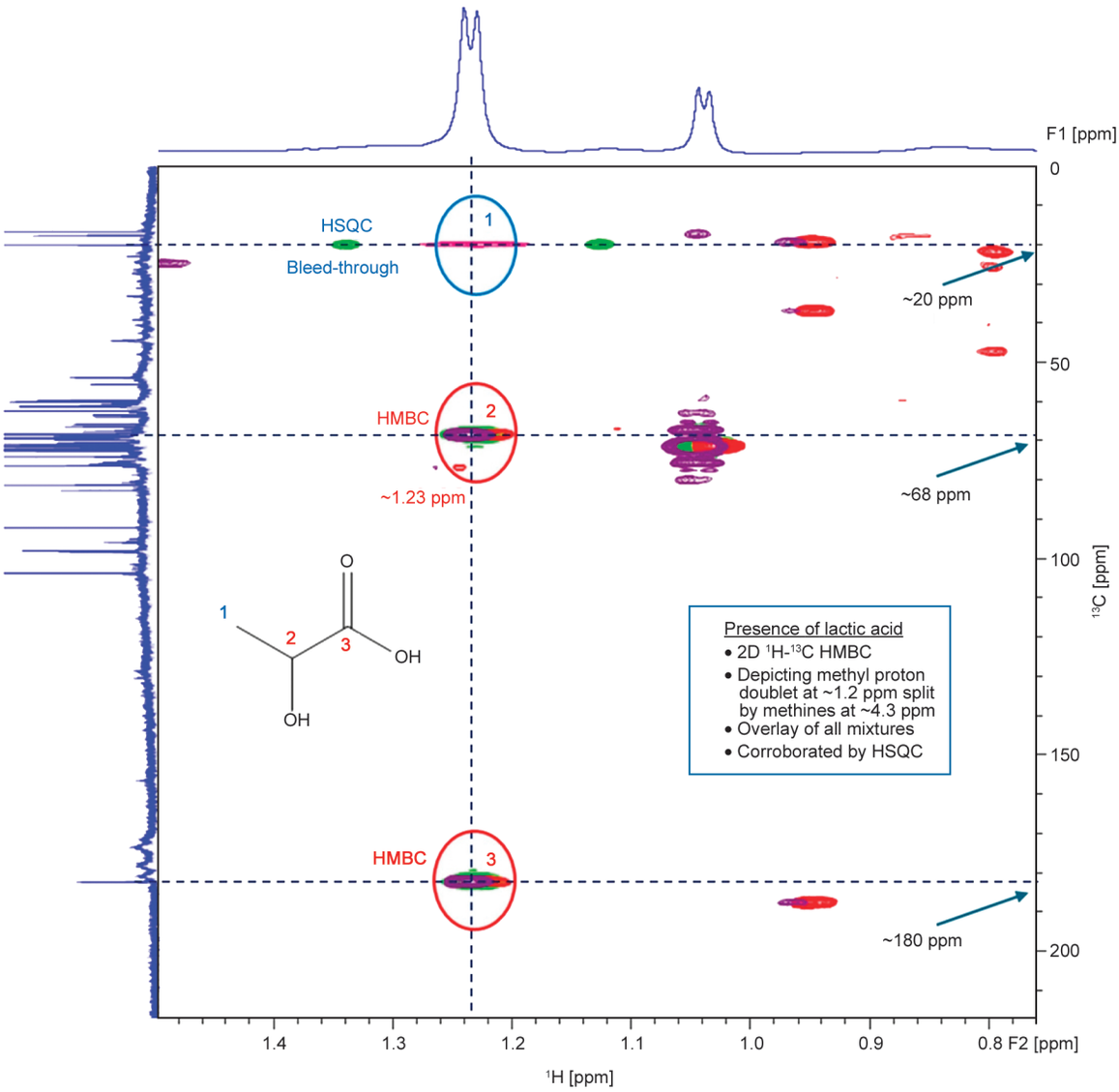

Figure 12. Overlay of 2D ^{1}H–^{13}C HMBC with bleed-through from HSQC (top cross-peaks) for all three extracts. Cross-peak assignments are consistent with the presence of lactic acid. Protons and carbons are color-coded in the structure inlay to correspond with circled cross-peaks.

^{1}H NMR peaks for citric acid were observed to undergo line narrowing, independent of the presence or absence of PAE.

NMR line widths for non-exchangeable aliphatic proton atoms are affected by molecular dynamics in solution [29]. For example, line broadening is often associated with incomplete averaging of chemical shift anisotropy (CSA) and dipolar interactions arising from slow molecular tumbling rates, leading to shorter spin-spin (T_2) relaxation times. Conversely, higher molecular tumbling rates lead to isotropic averaging of CSA and dipolar interactions, and hence to longer T_2 relaxation times and narrower line widths.

Molecular tumbling rates can be affected by the viscosity of the liquid medium and by intermolecular associations that impede molecular motion, such as hydrogen bonding, or by chemical changes that lead to changes in molecular weight or solubility. In this instance, if the viscosity of the medium were responsible for line broadening, then all ^{1}H NMR peaks would have exhibited similar degrees of line broadening. Given that the citric acid peaks in the extract from the as-received soy flour were selectively broadened while the other peaks remained narrow, it follows that the mobility of citric acid was selectively inhibited. Further, the inhibition in molecular mobility was removed upon hot-pressing, as evidenced

by line narrowing in the extracts from the hot-pressed samples.

Similar line broadening effects have been observed for citric acid when combined with L-arginine in an aqueous solution [30]. The broadening was attributed to a hydrogen bonding association, which leads to slower rotational molecular diffusion, longer T_2 relaxation times, and broader NMR peaks. Given that water-soluble peptides were extracted from the as-received soy flour as evidenced by the presence of an amide-I band in the soluble extract, and given that carbonyl amide-I bands were not observed in the low-haze extracts from the hot-pressed films, it follows that a similar type of association between peptides and citric acid may have been responsible for the ^{1}H NMR line broadening of citric acid in the soy flour extract. This hypothesis is indeed consistent with the line narrowing that was observed to occur in the extracts from the hot-pressed adhesive films, where soluble peptides were absent.

3.6. Implications of lactic acid

The formation of lactic acid on a laboratory scale suggests that it can also be formed during industrial-scale preparations of wood composites, particularly in processes that employ batch mixing of soy flour with water. Given that lactic acid can form from the fermentation of carbohydrates in soy, and given that lactic acid itself can subsequently lead to the chain scission of soy proteins [22], it is possible that the presence of lactic acid could lead to the formation of lower molecular peptide segments during the manufacturing process, some of which might be water-soluble. In one regard, this could be a positive attribute during the wood composite manufacturing process, because the presence of water-soluble proteins could lead to improved wood penetration and to improved adhesion through crosslinking with additives like citric acid and PAE.

However, the presence of lactic acid could also lead to negative effects during end-use. Given that the cured soy adhesives contain carbohydrates like those found in 67-3 and 67-4, and given that these carbohydrates are known to aggregate at the adhesive/ wood interface [8], it is plausible that the formation of lactic acid during end-use (*e.g.*, upon the exposure of wood laminates to moisture) could lead to further carbohydrate fermentation and therefore, to faster dissolution of the carbohydrate-rich weak boundary layers.

3.7. PAE solution chemistry

The observations presented thus far show that the as-received soy flour contains water-soluble peptides, carbohydrates, and carboxylic acids that are available to undergo thermally induced reactions to yield new water-soluble and water-insoluble reaction products. When PAE is added to the mixture, several additional reaction opportunities arise.

PAE is a water-soluble oligomer comprised of adipate ester linkages, secondary amide linkages, and 3-hydroxy-azetidinium (AZR) groups. The electrophilic AZR groups are known to undergo reactions with nucleophilic amines [1] and with carboxylic acid groups such as those found in carboxymethyl cellulose (CMC) [31]. Given that the water-soluble fraction of soy flour contains lactic acid, citric acid, and peptides, it follows that any of these water-soluble components would be available to react directly with PAE to yield a variety of water-soluble as well as water-insoluble reaction products.

As shown previously in Figure 1, a water-soluble component consistent with the structure of either adipic acid or an adipate adduct appeared in the extract from the 67-3 soy flour adhesive made with PAE. This was confirmed by 2D COSY, ^{1}H–^{13}C HSQC, and ^{1}H–^{13}C HMBC results as shown in Figure 13–15, respectively.

The appearance of the adipic structure could be related to the presence of unreacted PAE. In fact, the 1D and 2D spectral results as presented here agree with those from previous 1D and 2D NMR studies of PAE in water [31]. However, PAE is also comprised of secondary amide linkages, as confirmed by previous FTIR studies on solid PAE films [31], which showed the presence of a characteristic amide-I carbonyl band at 1635 cm^{-1}. By contrast, as shown in Figures 4 and 10, the amide-I band for PAE was not present in the FTIR spectrum of the 67-3 extract. This implies that the adipic structure in the 67-3 extract is not associated with unreacted PAE.

It is also possible that the adipic structure in the 67-3 extract is associated with an ester, formed through a reaction between PAE and a carboxylic acid. In fact, previous studies of reactions between PAE and carboxy methyl cellulose have revealed the disappearance of the amide-I band, accompanied by the appearance of an ester linkage at 1742 cm^{-1} [31]. However, as mentioned previously and as shown in Figure 4, there were no ester linkages in the FTIR spectrum of the 67-3 extract. Given the absence of

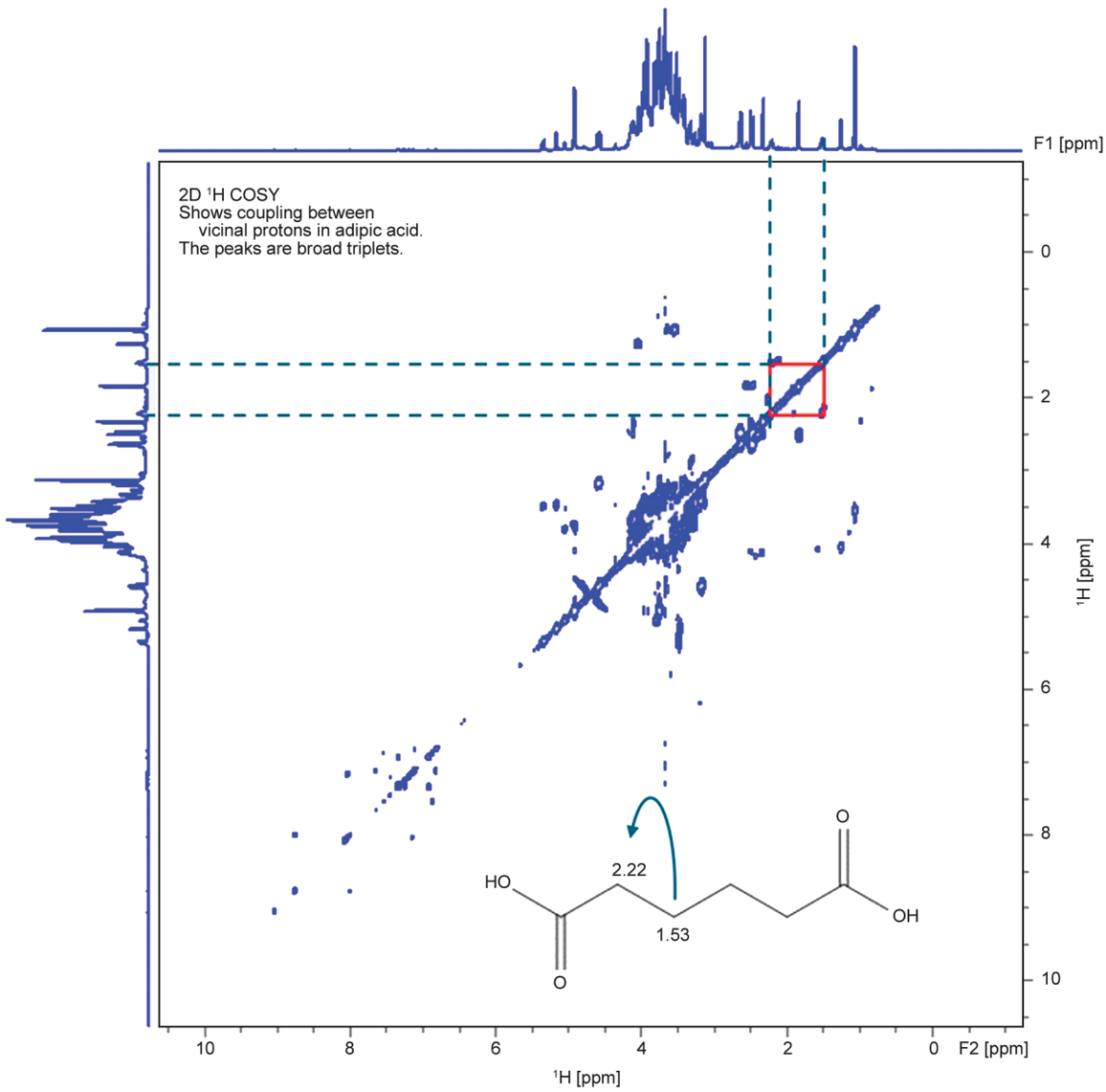

Figure 13. 2D ^{1}H–^{1}H COSY NMR spectrum for the filtered water-soluble extract from 67-3 showing cross peaks with correlated aliphatic ^{1}H–^{1}H coupling between 2.22 and 1.53 ppm, consistent with the presence of adipic acid.

ester and amide linkages, the remaining possibility is that a portion of the PAE must have become hydrolyzed either before and/or during the hot-press lamination process to yield adipic acid. Indeed, the presence of a band at 1608 cm^{-1} is consistent with the asymmetric stretch of a water-soluble carboxylate salt [31]. PAE chain scission, which would accompany hydrolysis, is also consistent with dynamic mechanical results as will be discussed below.

3.8. Dynamic mechanical analysis results

DMA anelastic spectral overlays for the 67-3 and 67-4 adhesive films are provided in Figure 16. These results show that PAE leads to plasticization under the process conditions employed in this study. When compared to the neat soy flour adhesive (67-4), the adhesive made with PAE (67-3) exhibited a lower effective glass transition temperature (T_g), a lower glassy state modulus, and a lower rubbery plateau modulus, consistent with qualitative comparisons as described earlier, and consistent with solid-state NMR results, as reported previously [8].

The plasticization effect was also accompanied by an increase in toughness as shown in Figure 17. The adhesive made with PAE exhibited higher stress and strain at break under constant strain rate conditions. The PAE film also exhibited a lower modulus, as gauged by the lower slope of the stress–strain curve. This was consistent with the lower storage modulus of the 67-3 film as measured dynamically at 1 Hz (Figure 16), and with qualitative trends as noted earlier.

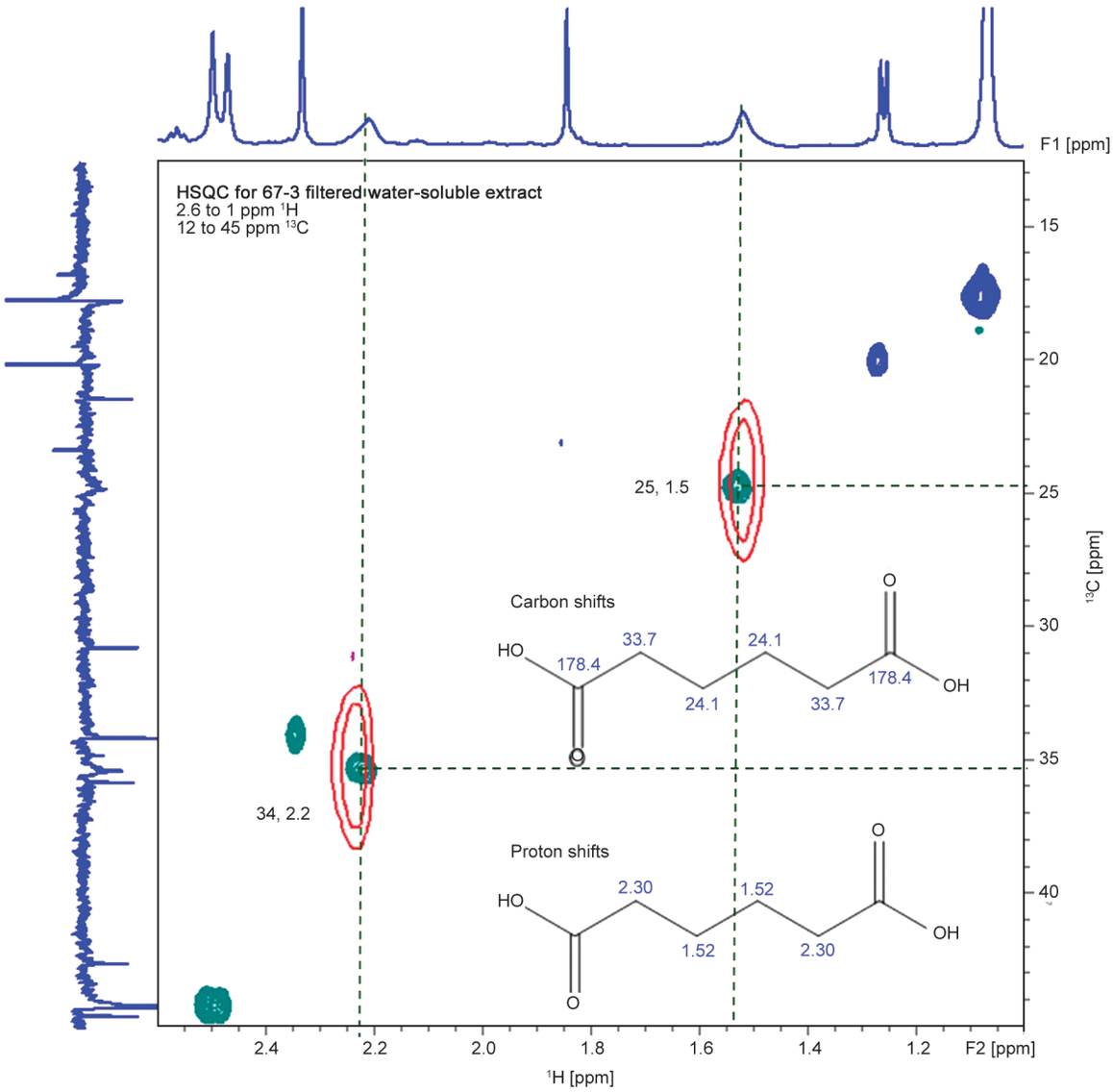

Figure 14. 2D ^{1}H–^{13}C HSQC NMR spectrum for the filtered water-soluble extract from 67-3 showing cross peaks with protons directly bonded to correlating carbon atoms, consistent with the presence of adipic acid.

Independently of the presence or absence of PAE, both adhesives also exhibited a well-defined rubbery plateau region, which is typical of a crosslinked polymer [32, 33]. The effective molecular weight between crosslinks (M_c) can be calculated from the rubbery plateau region with Equation (1), where E'_r represents the rubbery plateau storage modulus, T_r represents the onset temperature of the rubbery plateau in Kelvin, R represents the gas constant, and D represents the density of the material [33]:

$$M_c = \frac{3DRT_r}{E'_r} \quad (1)$$

The effective molecular weight between crosslinks was higher in the presence of PAE, which is indicative of a more loosely crosslinked network (*i.e.*, lower crosslink density). The parameters used to calculate the relative M_c are provided in Table 1 together with the other mechanical results.

Crosslinking in the absence of PAE is not surprising, especially given that soy proteins can react with other components like carbohydrates and citric acid to yield crosslinked structures [25–27]. Moreover, crosslinking in the presence of PAE is also not surprising, especially because soy flour contains reactive peptides, as noted earlier. However, a PAE-induced plasticization effect, accompanied by a reduction in apparent crosslink density, necessitates a deeper analysis.

From a simple two-component blending perspective, it is possible that because of PAE's low T_g [31], it could behave as a plasticizing reactive diluent,

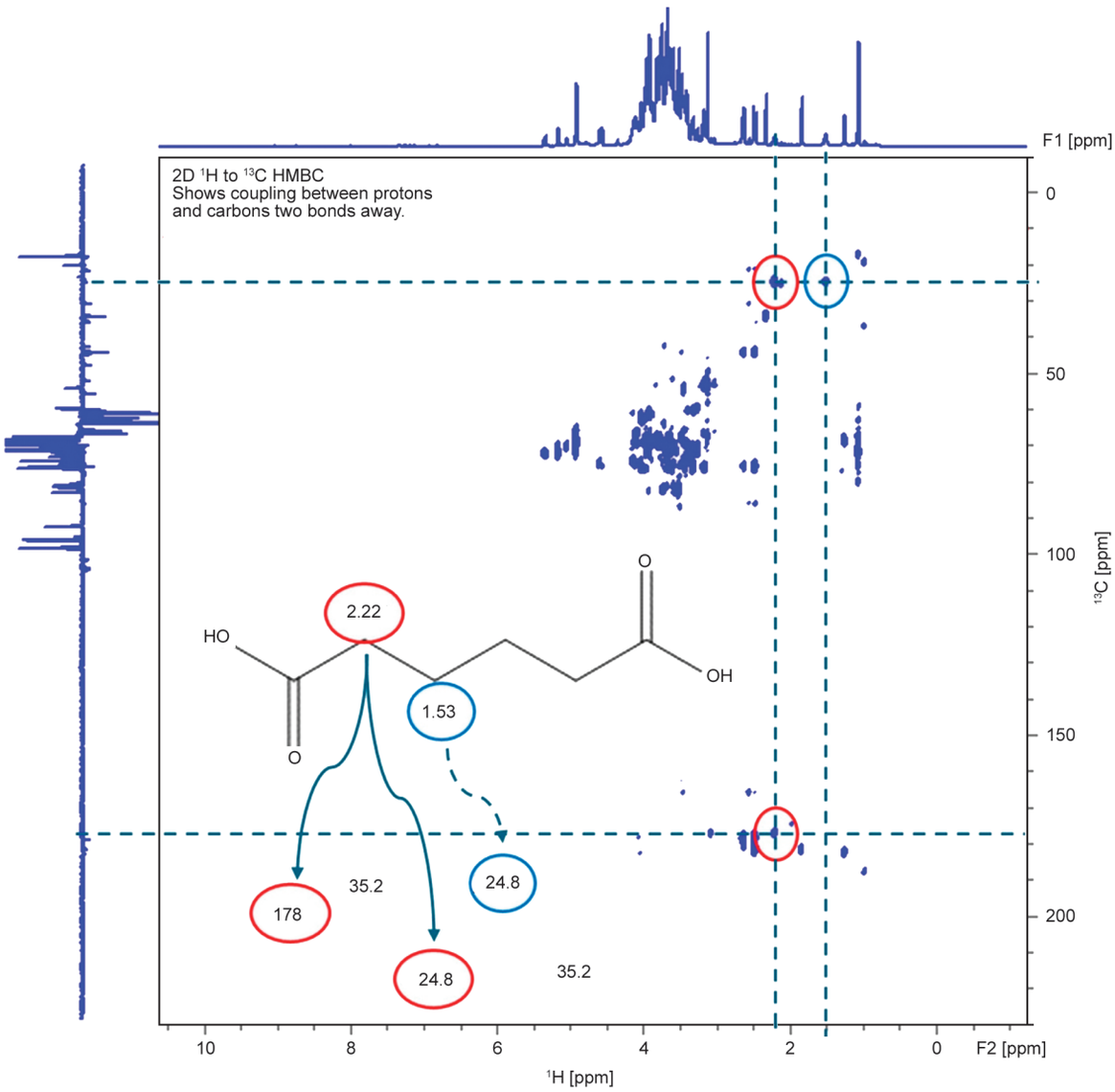

Figure 15. 2D ^{1}H–^{13}C HMBC NMR spectrum for the filtered water-soluble extract from 67-3 showing cross peaks with protons correlating through space to carbon atoms as denoted, consistent with the presence of adipic acid.

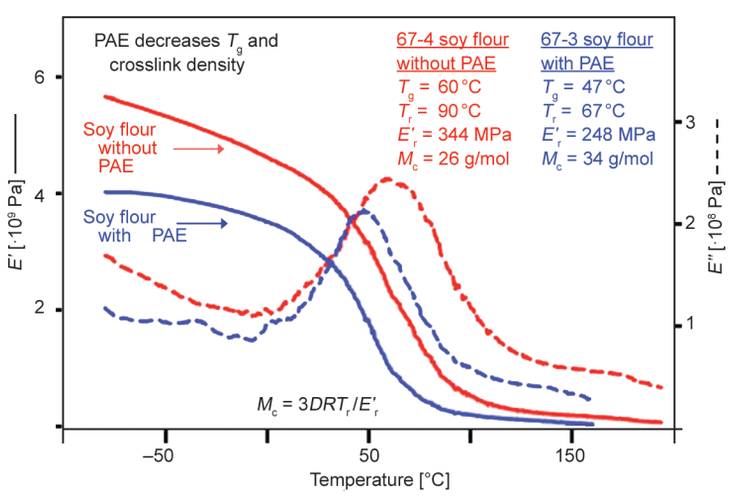

Figure 16. DMA storage (E') and loss (E'') moduli for 67-3 and 67-4, measured at 1 Hz, 5 °C/min.

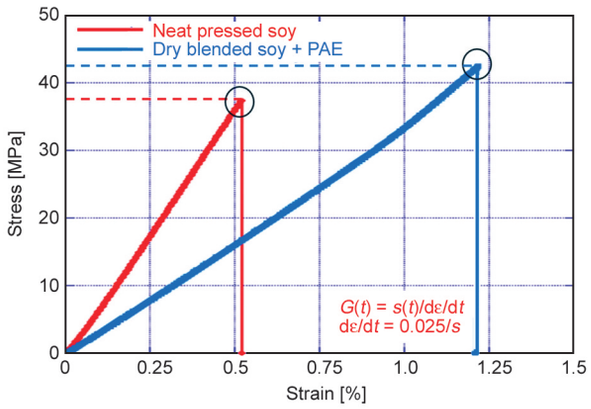

Figure 17. Constant strain rate results for the hot-pressed dry blends depicting shear stress and strain at break. Samples were run isothermally at 30 °C with a constant strain rate of 0.025% per second to the point of failure (circled).

Table 1. DMA fixed-frequency and constant strain rate results, including the calculated relative molecular weight between crosslinks M_c. Density (D) was assumed to be 1 g/cm^3 for both adhesives.

		67-4 soy flour without PAE	67-3 soy flour with PAE
T_r	[°C]	90	67
E'_r	[MPa]	344	248
Relative M_c	[g/mol]	26	34
T_g from E'' maximum	[°C]	60	47
Ultimate shear stress, 30 °C	[MPa]	37.5	42.5
Strain at break, 30 °C		0.54	1.23
Shear modulus, G, 30 °C	[MPa]	69.4	34.6

particularly if crosslinking reactions were to be somehow minimized or inhibited. For example, previous differential scanning calorimetry studies of neat PAE films revealed apparent T_g values ranging from near 0 °C for ambient-dried films, to approximately 60 °C for neat films that were heated at 105 °C for 24 h [31]. The T_g values were observed to correlate with the degree of PAE self-crosslinking reactions, which were maximized at higher temperatures in neat films [31]. From a reactive diluent perspective, the use of PAE at a diluted level in a soy flour adhesive (4% in this case) would favor a lower degree of PAE self-crosslinking, especially when cured under relatively mild conditions (*i.e.*, 130 °C for 14 min in this case). Thus, depending on the degree of its reaction with other components, PAE could indeed contribute to a reduction in T_g, at least from a simple blending perspective.

It is also conceivable that competitive reactions between PAE and the water-soluble components from soy flour could be responsible for the observed decrease in crosslink density and T_g. In the absence of PAE (sample 67-4), carbohydrates, lactic acid and citric acid are each independently capable of reacting with proteins [14, 15, 26, 27], and carbohydrates are also independently capable of reacting with citric acid [28]. In addition, because citric acid is trifunctional, multiple co-reaction products are also possible. For example, polypeptide chains could become linked to carbohydrate chains via citric acid bridges. This means that in the absence of PAE, there are several possible reaction pathways that can lead to a crosslinked network. When PAE is added to the mixture (sample 67-3), the number of possible reaction pathways is significantly increased. For example, PAE can independently react with proteins, with lactic acid, with citric acid and with carbohydrates that are functionalized with carboxylic acids [1, 5, 7, 31]. Moreover, because PAE is comprised of multiple AZR groups, it can also co-react with each of these species, leading to a multitude of possible reaction products. This means that in addition to all the competitive reactions that can occur in the absence of PAE, several more permutations are possible in the presence of PAE. As described below, many of these reaction products would have the potential to reduce T_g and crosslink density.

For example, as shown in Figure 18, reactions between PAE and mono-functional carboxylic acids [31] like lactic acid could lead to the formation of terminally grafted PAE chains instead of traditional crosslinked structures [1]. The appearance of these types of structures would be consistent with the disappearance of water-soluble peptides as observed via NMR and FTIR, and also with the reduction in the relative concentration of lactic acid as observed via ^{1}H NMR. An increase in free volume associated with an increase in the number of terminal (non-crosslinked) PAE chain ends would be consistent with the decrease in T_g [32], as observed via DMA. Simultaneously, chain termination with lactic acid would also reduce the number of AZR groups available for additional crosslinking reactions.

PAE is also a low molecular weight water-soluble resin with multiple AZR functional groups, characterized in one account as having a number average molecular weight ranging between approximately 6000 and 10 000 g/mol [31]. By contrast, citric acid is a smaller trifunctional molecule with a molecular weight of 192 g/mol. Thus, based on size differences alone, PAE also has the potential to reduce crosslink

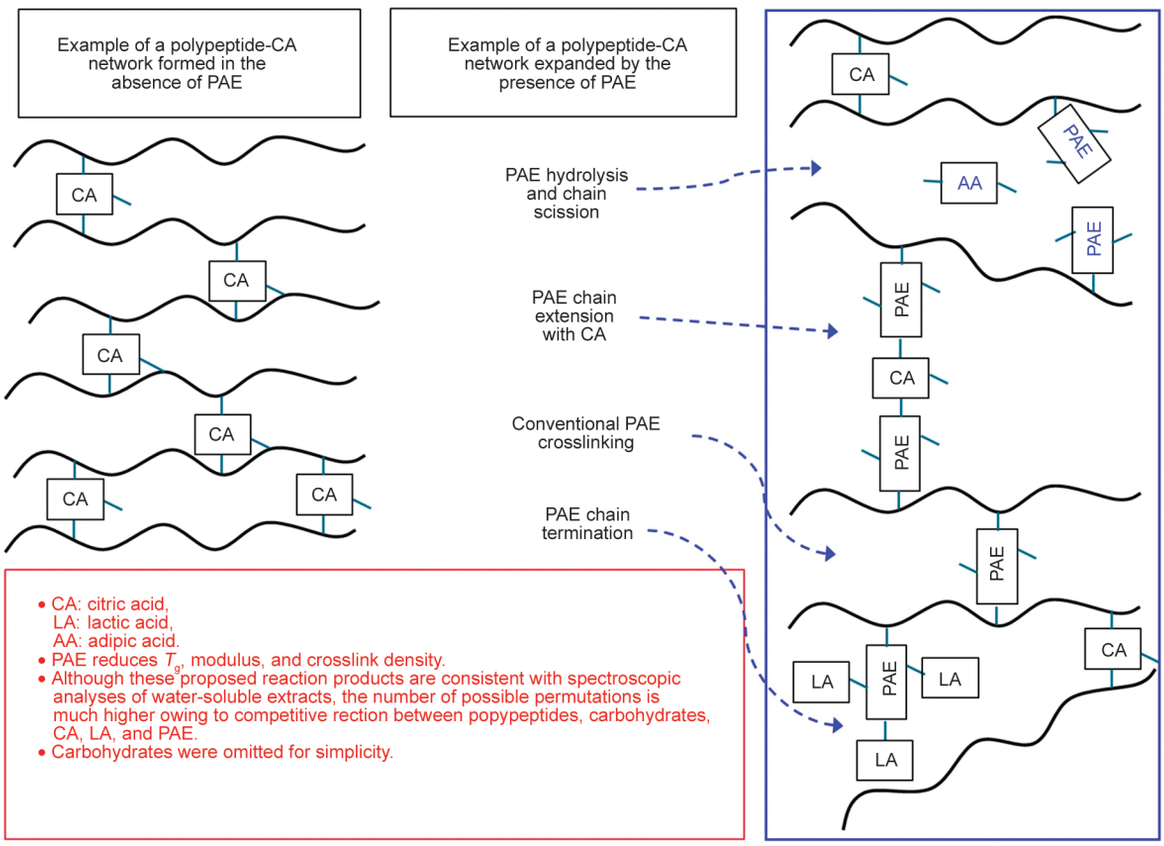

Figure 18. Examples of crosslinked polypeptide networks formed in the absence and in the presence of PAE. A plethora of crosslinked water-insoluble reaction products can arise from competitive reactions between PAE and water-soluble components in soy flour. A few possibilities are exemplified here in this simple two-dimensional depiction, based on consistency with spectroscopic and DMA results. The proposed reaction products were limited to those derived from specific water-soluble soy flour components, including polypeptide chains (represented by wavy black lines), lactic acid (LA) and citric acid (CA). Each soluble reactant has the potential to react with PAE to yield the types of structures as depicted, including traditional PAE crosslinks, PAE crosslinks that are chain-extended with CA, and LA-terminated PAE grafted structures. In addition, PAE hydrolyzes to yield adipic acid (AA), which can lead to PAE chain scission (shown in blue), and plasticization by AA. Although soluble carbohydrates can also participate in various reactions (*e.g.*, CA bridging reactions between PAE, proteins and carbohydrates), they were omitted from this description for reasons described in the text.

density by expanding the distance between adjacent polypeptide chains through the formation of direct crosslinks (Figure 18).

It is also possible for the crosslinked network to become chain-extended through competitive reactions between citric acid and PAE. If the 67-4 adhesive (*i.e.*, without PAE) is used as the baseline example of peptide crosslinking with citric acid alone [25–27], the addition of PAE could lead to additional structures, in part because citric acid has the capacity to independently react with PAE [31], with proteins [25–27] and with carbohydrates [28]. For example, as shown in Figure 18, a crosslinked network formed through the reaction of polypeptides with citric acid would lead to a crosslink density defined in part by the intermolecular distance associated with the citrate crosslink junctures between adjacent peptide chains. If PAE is added to this network, competitive reactions between PAE and citric acid could lead to a larger distance between crosslinked peptide chains, and even to the formation of branched structures. The formation of each of these types of structures would be consistent with the decrease in crosslink density as observed via DMA, and with the disappearance of water-soluble peptides as observed via NMR and FTIR.

As noted previously, carbohydrates can also participate in competitive reactions with proteins and citric acid [14, 15, 28]. For example, as shown in Figure 5, the water-soluble carbonyl amide that was originally present in the as-received soy flour was thermally transformed in the absence of PAE (sample 67-4) to yield an insoluble proteinaceous material, suggestive

of a possible Maillard reaction product [14]. The co-reactivity of citric acid with proteins [25–27] and with carbohydrates [28] can also lead to bridged networks comprised of polypeptide chains linked to carbohydrate chains. In addition, because PAE can also independently react with carboxylic acids [31], it may be possible for PAE to co-react with both proteins and carbohydrates via citric acid bridging to yield a crosslinked lattice structure that is much more complex than the simple polypeptide lattice depicted in Figure 18. However, the spectroscopic data has shown that unlike the water-soluble polypeptides, heat-modified carbohydrates remained water-soluble after processing, independently of the presence or absence of PAE. This suggests that PAE has a lower propensity to react with the soluble carbohydrates in soy flour, and a greater propensity to react with other soluble components. This hypothesis is consistent with previous observations, where carbohydrates became concentrated at the wood/adhesive interface in composites made with and without PAE [8], and where an anomeric carbon associated with carbohydrates disappeared from the solid state ^{13}C NMR spectra of the same crosslinked reaction products (*i.e.*, 67-3 and 67-4) after water extraction, independently of the presence or absence of PAE [8].

Finally, given that a structure consistent with an adipic acid salt was observed in the water-soluble extract from 67-3 via NMR and FTIR, it follows that PAE molecules were cleaved by hydrolysis. As mentioned earlier, the hydrolysis of PAE would lead to PAE chain scission. This in turn could transform the PAE crosslinked chains into grafted side-chain structures (Figure 18), which would lead to an increase in free volume [32], consistent with the observed decrease in T_g and crosslink density.

Plasticization can also be affected by the morphology of the adhesive and by the composition of the water-soluble fraction. For example, previous solid-state NMR studies of the neat adhesives [8] revealed differences in average rotating frame proton spin lattice relaxation rates ($^1HT_{1\rho}$) as measured through ^1H–^{13}C cross polarization under ambient conditions. The results showed that when PAE was used as a crosslinking additive, the water-soluble components appeared to plasticize the adhesive matrix [8]. The enhanced plasticization imparted by the presence of the water-soluble fraction might indeed be related to the presence of adipic acid (Figure 18), which could function as a plasticizer for carbohydrates in the water-soluble phase of the adhesive, analogous to the way adipate esters function as plasticizers for analogous water-insoluble polymers with anomeric protons [34].

3.9. Adhesion implications

It is well known that the mechanism of adhesion between component members in composite structures is influenced by interfacial contributions (*e.g.*, surface wetting and interpenetration between the components), and by bulk mechanical property contributions (*e.g.*, viscoelastic and energy-absorbing characteristics of the individual component members) [35, 36]. Moreover, good interfacial penetration between members can lead to phase mixing at the boundary and the development of a mixed interphase with its own unique set of mechanical properties [37].

With respect to PAE's interfacial contributions to adhesion in soy-bonded wood composites, previous FTIR studies have shown that water-soluble components (*e.g.*, carbohydrates) preferentially penetrate the wood adherend to form moisture-sensitive boundary layers that become the loci of near-interfacial failures, independently of the presence or absence of PAE [8]. Thus, when composites are exposed to water, the water-soluble interfacial layer appears to become the weakest mechanical link in the adhesive system [8]. Based on the solution NMR results of this study, it appears that apart from adipic acid in the adhesive made with PAE, the water-soluble extracts from the post-cured soy flour adhesives are comprised of similar water-soluble components (*i.e.*, heat-modified carbohydrates, citric acid, and lactic acid), suggesting that the improvements in wet-strength adhesion that arise from the use of PAE [1, 4, 5, 7] are probably not related to PAE-induced compositional differences within the moisture-sensitive boundary layer. Instead, given that PAE plasticizes and toughens the bulk adhesive, it follows that the improvement in wet-strength adhesion from PAE most likely arises from its ability to impart better viscoelastic energy absorption and bulk stress dissipation within the bulk adhesive, which reduces the appearance of stress concentrates near the adhesive/adherend interface [36].

4. Conclusions

Based on the results of fixed-frequency DMA and constant strain rate measurements, PAE plasticized the bulk soy flour adhesive, resulting in a lower

modulus, in a lower T_g, and in a higher stress and strain to break. In addition, PAE was also observed to decrease relative crosslink density, as evidenced by a lower rubbery plateau modulus, and by a lower plateau onset temperature. Although these findings corroborate our previous solid-state NMR studies [8], they also present new questions about PAE's traditional role as a crosslinking agent [5], implying instead that PAE's role is more akin to that of a reactive plasticizer.

These unexpected results imply that PAE's ability to improve the moisture resistance of laminated wood composites [1, 4, 5, 7] cannot be attributed to crosslinking alone. Instead, in keeping with our previously posed hypothesis [8], it is more likely that plasticization from PAE leads to enhanced viscoelastic energy absorption and stress dissipation during water-soaking and drying cycles, thereby minimizing the occurrence of interfacial shear stress concentrates that would otherwise lead to failures within the weak boundary layer.

Although PAE's traditional role as a multifunctional crosslinking agent for proteins and carbohydrates [1, 4, 5, 7] cannot be entirely discounted, the results of the present study show that traditional crosslinking is only one of several possible reaction pathways by which PAE reacts with the components of soy flour. For example, given that proteins, lactic acid, citric acid, and carboxylic acid–functionalized carbohydrates are each independently capable of reacting with PAE [1, 5, 7, 31]; and given that carbohydrates, lactic acid, and citric acid are also each independently capable of reacting with proteins [25–28], and given that carbohydrates can independently react with citric acid [28], it follows that competitive reactions between all these species can lead to a plethora of reaction products, several of which have the potential to reduce T_g and reduce crosslink density by inhibiting network formation. This means that the previously assumed model of PAE crosslinking in soy flour adhesives [1] is overly simplistic, and that the true number of reaction pathways is much more extensive than previously assumed.

In fact, post-cure analyses of adhesive extracts revealed that the water-soluble peptides from soy flour were no longer soluble after thermal curing, indicating that they indeed react to yield water-insoluble reaction products, independently of the presence or absence of PAE. Simultaneously, the disappearance of the soluble polypeptides was also accompanied by a change in the ^{1}H NMR linewidth for citric acid protons, consistent with a scenario whereby soluble peptides and citric acid can participate in crosslinking reactions [25–28] both in the presence and in the absence of PAE, and where competitive reactions also have the potential to occur between citric acid, water-soluble peptides and AZR groups in the presence of PAE.

Similarly, ^{1}H NMR also revealed that the disappearance of the soluble polypeptides was accompanied by a reduction in the relative intensity of lactic acid protons, independent of the presence or absence of PAE. This is consistent with the possibility that lactic acid can react with peptides [22] both in the presence and in the absence of PAE. Moreover, lactic acid could also competitively participate in direct reactions with AZR groups in the presence of PAE [31], leading to terminal reaction products, which would interfere with PAE's ability to form crosslinks between adjacent macromolecular chains. Indeed, PAE chain termination with lactic acid, and chain extension with citric acid would be consistent with the observed decrease in crosslink density and T_g.

Equally important, the appearance of adipic acid in the NMR spectra of the post-cured extract from the PAE-cured adhesive is indicative of PAE hydrolysis and chain scission. This process likely contributes to incomplete network development through the conversion of interchain crosslinked structures to pendent graft-like structures (Figure 18). This could also lead to a decrease in crosslink density and to plasticization. Moreover, the resulting hydrolysis product itself (*i.e.*, adipic acid) could also function as a plasticizer on its own.

^{1}H NMR and FTIR analyses of post-cured extracts also revealed the presence of heat-modified, water-soluble carbohydrates, independently of the presence of PAE. These components were identifiable with those previously found to constitute the moisture-sensitive weak boundary layer associated with wet delamination failure in wood composites [8]. Although proteins can react with carbohydrates to yield insoluble crosslinked structures via the Maillard reaction [14, 15], these particular carbohydrates remained inherently water-soluble after cure, independently of the presence of PAE. Thus, regardless of the improvements in moisture resistance imparted by PAE [1, 4, 7], and regardless of the exact mechanistic reasons for the improvements (*e.g.*, viscoelastic energy absorption and stress dissipation), the

weak link in the soy flour adhesive system continues to be a moisture-sensitive weak boundary layer comprised of soluble carbohydrates [8], augmented by the presence of soluble carboxylic acid structures as indicated by the present study.

Thus, to improve the moisture resistance of soy-based adhesives in wood composites, and to ultimately achieve the degree of moisture resistance exhibited by other adhesives like PMDI and PF [1, 2, 9, 10], we first have to develop a better way to render the water-soluble components insoluble after thermal processing, perhaps through targeted crosslinking, while still enabling those components to penetrate the wood adherends during the manufacturing process (*i.e.*, before crosslinking is complete, and hence before insolubility is rendered), so as to allow for the development of a well-formed interphase comprised of wood, interpenetrated by a network of crosslinked adhesive components. A curing construct of this type would be analogous to that embodied by other thermosetting systems, including PF and PMDI adhesives [9, 10]. The second challenge from a manufacturing perspective would be to maintain economic viability. Thus, the ideal crosslinking agent(s) and/or co-reactants would likely have to react with the water-soluble components within time and temperature windows that are commensurate with those of fast-throughput manufacturing processes.

From a formulation and polymer physics perspective, plasticization can also be used as a physical lever to enhance adhesion strength, where viscoelastic energy absorption and bulk stress dissipation within the bulk adhesive can be leveraged to reduce the appearance of stress concentrates near the adhesive/adherend interface [36]. Although PAE appears to impart this function, there are many other types of plasticizers that might also work in this regard. Examples could include reactive and non-reactive types, including natural product-based plasticizers like those comprised of glycerol esters with lactic acid [38].

Given the confirmed presence of reactive amine functional groups together with citric acid and carbohydrates in the water phase of dispersed soy flour adhesives, we have conceptualized a chemically feasible path forward whereby fast-reacting, electrophilic crosslinking reagents (*e.g.*, modified isocyanates and others) could be used to react with the available water-soluble moieties in soy flour (*i.e.*, amines, hydroxyls, and carboxylic acid groups) to yield water-insoluble reaction products. The goal of this endeavor will be to improve the moisture resistance of the moisture-sensitive weak boundary layer [8] through targeted crosslink chemistry. If successful, this would not only assist in improving the moisture resistance of the moisture-sensitive weak boundary layer, but it would also provide a pathway for facile crosslinking reactions, without having to compromise manufacturing throughput rates, and without having to rely upon the use of higher processing temperatures and/or higher-cost SPIs.

Acknowledgements

We thank the United Soybean Board for funding this research (Project Number: 25-101-D-C-1-A); Columbia Forest Products for providing the 200/70 soy flour, PAE resin, and wood veneers; Justin Crouse of The University of Maine advanced structures and composites center, Orono, ME, for assistance with DMA measurements; and Dr. James Rocca of the University of Florida for assistance with NMR studies. A portion of this work was performed at the McKnight brain institute at the national high magnetic field laboratory's AMRIS facility, supported by NSF cooperative agreement DMR-2128556 and the state of Florida.

References

[1] Frihart C. R., Birkeland M. J.: Soy properties and soy wood adhesives. in 'Soy-based chemicals and materials' (ed.: Brentin R. P.) American Chemical Society, Washington, Vol. 1178, 167–192 (2014). https://doi.org/10.1021/bk-2014-1178.ch008

[2] Pizzi A., Papadopoulos A. N., Policardi F.: Wood composites and their polymer binders. Polymers, **12**, 1115 (2020). https://doi.org/10.3390/polym12051115

[3] Jang Y., Li K.: An all-natural adhesive for bonding wood. Journal of the American Oil Chemists Society, **92**, 431–438 (2015). https://doi.org/10.1007/s11746-015-2610-y

[4] Varnell D. F., Spraul B. K., Evans M. A.: Adhesive compositions. U.S. Patent 8,399,544 B2, United States (2013).

[5] Kallakas H., Plaza N., Crooks C., Turner D., Gargulak M., Arvanitis M. A., Frihart C. R., Hunt C. G.: Effect of protein surface hydrophobicity and surface amines on soy adhesive strength. Polymers, **16**, 202 (2024). https://doi.org/10.3390/polym16020202

[6] Bainy E. M., Tosh S. M., Corredig M., Poysa V., Woodrow L.: Varietal differences of carbohydrates in defatted soybean flour and soy protein isolate by-products. Carbohydrate Polymers, **72**, 664–672 (2008). https://doi.org/10.1016/j.carbpol.2007.10.008

[7] Lorenz L., Birkeland M., Daurio C., Frihart C. R.: Soy flour adhesive strength compared with that of purified soy proteins. Forest Products Journal, **65**, 26–30 (2015). https://doi.org/10.13073/FPJ-D-13-00020

[8] Marcinko J. J., Parker A. A.: Spectroscopic characterization of the chemical changes occurring in soy wood composite adhesives when exposed to moisture. Forest Products Journal, **74**, 143–150 (2024). https://doi.org/10.13073/FPJ-D-23-00063

[9] Gruver M. T., Brown N. R.: Penetration and performance of isocyanate wood binders on selected wood species. BioResources, **1**, 233–247 (2006). https://doi.org/10.15376/biores.1.2.233-247

[10] Gindl W., Schöberl T., Jeronimidis G.: The interphase in phenol–formaldehyde and polymeric methylene diphenyl-di-isocyanate glue lines in wood. International Journal of Adhesion and Adhesives, **24**, 279–286 (2004). https://doi.org/10.1016/j.ijadhadh.2003.10.002

[11] Field L. D., Li H. L., Magill A. M.: Organic structures from 2D NMR spectra. Wiley, Hoboken (2015).

[12] Ye G., Zhang J., Xu X., Zeng C., Ye Q., Wang Z.: Comparative analysis of water-soluble polysaccharides from *Dendrobium* second love 'tokimeki' and *Dendrobium nobile* in structure, antioxidant, and anti-tumor activity *in vitro*. International Journal of Molecular Sciences, **24**, 10361 (2023). https://doi.org/10.3390/ijms241210361

[13] Wishart D. S., Knox C., Guo A. C., Eisner R., Young N., Gautam B., Hau D. D., Psychogios N., Dong E., Bouatra S., Mandal R., Sinelnikov I., Xia J., Jia L., Cruz J. A., Lim E., Sobsey C. A., Shrivastava S., Huang P., Liu P., Fang L., Peng J., Fradette R., Cheng D., Tzur D., Clements M., Lewis A., de Souza A., Zuniga A., Dawe M., Xiong Y., Clive D., Greiner R., Nazyrova A., Shaykhutdinov R., Li L., Vogel H. J., Forsythe I.: HMDB: A knowledgebase for the human metabolome. Nucleic Acids Research, **37**, D603–D610 (2009). https://doi.org/10.1093/nar/gkn810

[14] El Hosry L., Elias V., Chamoun V., Halawi M., Cayot P., Nehme A., Bou-Maroun E.: Maillard reaction: Mechanism, influencing parameters, advantages, disadvantages, and food industrial applications: A review. Foods, **14**, 1881 (2025). https://doi.org/10.3390/foods14111881

[15] Yi Y., Han M-M., Huang F., Wang L-M., Min T., Wang H-X.: Effects of a lysine-involved Maillard reaction on the structure and *in vitro* activities of polysaccharides from longan pulp. Molecules, **24**, 972–986 (2019). https://doi.org/10.3390/molecules24050972

[16] Silverstein R. M., Webster F. X., Kiemle D. J., Bryce D. L.: Spectrometric identification of organic compounds. Wiley, Hoboken (2014).

[17] Frihart C. R., Satori H.: Soy flour dispersibility and performance as wood adhesive. Journal of Adhesion Science and Technology, **27**, 2043–2052 (2013). https://doi.org/10.1080/01694243.2012.696948

[18] Campbell I. D., Dwek R. A.: Biological spectroscopy. Benjamin Cummings, Menlo Park (1984).

[19] Wishart D. S., Sykes B. D., Richards F. M.: The chemical shift index: A fast and simple method for the assignment of protein secondary structure through NMR spectroscopy. Biochemistry, **31**, 1647–1651 (1992). https://doi.org/10.1021/bi00121a010

[20] Perkins E. G.: Composition of soybeans and soybean products. in 'Practical handbook of soybean processing and utilization' (ed.: Erickson D. R.) Academic Press and AOCS Press, Amsterdam, 9–28 (1995). https://doi.org/10.1016/B978-0-935315-63-9.50006-1

[21] Hansen P. E., Vakili M., Kamounah F. S., Spanget-Larsen J.: NH stretching frequencies of intramolecularly hydrogen-bonded systems: An experimental and theoretical study. Molecules, **26**, 7651 (2021). https://doi.org/10.3390/molecules26247651

[22] Ogodo A. C., Ugbogu O. C., Onyeagba R. A.: Variations in the functional properties of soybean flour fermented with lactic acid bacteria (LAB)-consortium. Applied Microbiology: Open Access, **4**, 141 (2018). https://doi.org/10.4172/2471-9315.1000141

[23] Chozhavendhan S., Aniskumar M., Santhaseelan C., Muthu Gayathri D., Sathya R., Shmugapriya K.: A review on citric acid production and its applications. International Journal of Pharmacy and Biological Sciences, **11**, 79–85 (2021). https://doi.org/10.21276/ijpbs.2021.11.2.9

[24] Behera B. C., Mishra R., Mohapatra S.: Microbial citric acid: Production, properties, application, and future perspectives. Food Frontiers, **2**, 62–76 (2021). https://doi.org/10.1002/fft2.66

[25] Rebezov M., Oboturova N., Statsenko E., Bachukin V., Katkova E., Khayrullin M., Neverova O., Zinina O.: Crosslinking methods for improving the properties of soy-protein based films for meat packaging: A review. Potravinarstvo Slovak Journal of Food Sciences, **17**, 635–648 (2023). https://doi.org/10.5219/1892

[26] Li Y., Yang Y.: Formaldehyde-free chemical and enzymatic crosslinking of plant proteins. Research Journal of Textile and Apparel, **15**, 1–8 (2011). https://doi.org/10.1108/RJTA-15-04-2011-B001

[27] Reddy N., Li Y., Yang Y.: Alkali-catalyzed low temperature wet crosslinking of plant proteins using carboxylic acids. Biotechnology Progress, **25**, 139–146 (2009). https://doi.org/10.1002/btpr.86

[28] Seligra P. G., Jaramillo C. M., Famá L., Goyanes S.: Biodegradable and non-retrogradable eco-films based on starch–glycerol with citric acid as crosslinking agent. Carbohydrate Polymers, **138**, 66–74 (2016). https://doi.org/10.1016/j.carbpol.2015.11.041

[29] Parker A. A.: Poly(vinylbutyral-*co*-vinyl alcohol) tacticity and aluminum oxide surface adsorption. Macromolecules, **27**, 7363–7368 (1994). https://doi.org/10.1021/ma00103a016

[30] Roda A., Santos F., Chua Y. Z., Kumar A., Do H. T., Paiva A., Duarte A. R. C., Held C.: Unravelling the nature of citric acid:L-arginine:water mixtures: The bifunctional role of water. Physical Chemistry Chemical Physics, **23**, 1706–1717 (2021). https://doi.org/10.1039/D0CP04992A

[31] Siqueira E. J., Salon M. B., Belgacem M. N., Mauret E.: Carboxymethylcellulose (CMC) as a model compound of cellulose fibers and polyamideamine epichlorohydrin (PAE)–CMC interactions as a model of PAE–fibers interactions of PAE-based wet strength papers. Journal of Applied Polymer Science, **132**, 42144 (2015). https://doi.org/10.1002/app.42144

[32] Ward I. M., Sweeney J.: Mechanical properties of solid polymers: Third edition. Wiley, New York (2012). https://doi.org/10.1002/9781119967125

[33] Landel R. F., Nielsen L. E.: Mechanical properties of polymers and composites. CRC Press, Boca Raton (1993). https://doi.org/10.1201/b16929

[34] Parker A. A., Hedrick D. P., Ritchey W. M.: NMR studies of plasticizer motions in a polymer matrix. Macromolecules, **25**, 3365–3368 (1992). https://doi.org/10.1021/ma00039a008

[35] Theocaris P. S.: Synergism phenomena between phases in composites: The mesophase. Colloid and Polymer Science, **265**, 461–480 (1987). https://doi.org/10.1007/BF01412500

[36] Guillemenet J., Bistac S., Schultz J.: Relationship between polymer viscoelastic properties and adhesive behaviour. International Journal of Adhesion and Adhesives, **22**, 1–5 (2002). https://doi.org/10.1016/S0143-7496(01)00027-6

[37] Koenig J. L.: Spectroscopy of polymers. Elsevier, New York (1999). https://doi.org/10.1016/B978-0-444-10031-3.X5000-2

[38] Shahir F. A., Ahmadi Z., Darvishi S. M. R.: Sustainable packaging: A comparative study on thermoplastic whey protein films with biodegradable plasticizers. Express Polymer Letters, **18**, 592–606 (2024). https://doi.org/10.3144/expresspolymlett.2024.44